Laser trapping of low refractive index colloids in a nematic liquid crystal

M. Škarabot,[1] M. Ravnik,[2] D. Babič,[2] N. Osterman,[2] I. Poberaj,[2] S. Žumer,[1,2] and I. Muševič[1,2,*]
[1]*J. Stefan Institute, Jamova 39, 1000 Ljubljana, Slovenia*
[2]*Faculty of Mathematics and Physics, University of Ljubljana, Jadranska 19, 1000 Ljubljana, Slovenia*

A. Nych, U. Ognysta, and V. Nazarenko
Institute of Physics, Prospect Nauki 46, Kyiv-22, 252022, Ukraine
(Received 6 April 2005; revised manuscript received 6 January 2006; published 23 February 2006)

We describe and analyze laser trapping of small colloidal particles in a nematic liquid crystal, where the index of refraction of colloids is smaller compared to the indices of the liquid crystal. Two mechanisms are identified that are responsible for this anomalous trapping: (i) below the optical Fréedericksz transition, the trapping is due to the anisotropic dielectric interaction of the polarized light with the inhomogeneous director field around the colloid, (ii) above the optical Fréedericksz transition, the optical trapping is accompanied by the elasticity-mediated interaction between the optically distorted region of a liquid crystal and the colloid. In the majority of the experiments, the trapping above the Fréedericksz transition is highly anisotropic. Qualitative agreement is found with a numerical analysis, considering the nematic director elastic distortion, dielectric director-light field coupling and optical repulsion due to low refraction index colloid in high index surroundings.

PACS number(s): 61.30.Hn, 61.30.Pq, 68.08.−p

I. INTRODUCTION

The long-range nature of the orientational order in liquid crystals is responsible for many fascinating optic, electro-optic, and mechanical properties of liquid crystals. Recently, there has been an increased interest in novel liquid crystalline systems such as the inverted nematic emulsions [1–3] and nematic liquid crystal colloids [4,5]. It has been observed that the presence of small particles of a regular shape (i.e., colloids, water droplets) in an otherwise homogeneous nematic host gives rise to new, anisotropic structural forces, not observable in any other isotropic host. Being of an anisotropic nature, the interactions between inclusions induce growth of unique self-assembled structures such as linear chains [1,3], two-dimensional (2D) hexagonal arrangements of particles at interfaces [4,5], or regular arrays of defects [6]. The unique combination of long-range anisotropic structural forces in liquid crystals and their electro-optic properties could, therefore, lead not only to new self-assembled structures for controllable photonic devices, but also to novel soft solids with unusual mechanical properties [7].

The nature of the interaction between objects in nematic liquid crystals has so far been studied both theoretically and experimentally. The theoretical studies have been concentrated mainly on two-body interactions, neglecting many-body corrections, and using either analytical [1,8–16] or fully numerical approach [17–21]. The analytical, in most cases, multipole-expansion approach, is expected to be valid in the far-field regime, i.e., at large interparticle separations, where the perturbation of the inclusions is small. In this picture, the object in a liquid crystal is considered as a static source of either a monopole, dipole, or quadrupole field that interacts in a pairwise manner with another object in its vicinity. This approach is, therefore, analogous to the multipole interaction picture in electrostatics and predicts $1/r^2$ structural force between two monopoles, $1/r^4$ structural force between two dipolarlike objects, and $1/r^6$ force between two topological quadrupoles. In comparison, a fully numerical approach [21], found a good agreement for two parallel dipoles generating $1/r^4$ attractive force; whereas, for two anti-parallel dipoles, the numerically calculated repulsive force was stronger than expected from analytical considerations, $1/r^3$. The clear theoretical argument for the breakdown of the analytical approach is not available at this time, but is an indication of its limited validity.

The experiments were so far mainly concentrated on the study of dipolar and quadrupolar interactions in nematic colloids. Poulin *et al.* [22] have observed $1/r^4$ dipolar attractive forces between 2.8 μm ferrofluid droplets in a nematic over a limited range of separation 9–18 μm. Yada *et al.* [23] have used laser tweezers to trap and measure forces between polystyrene colloids of micron size in the low-index nematic. They have found $1/r^4$ attraction in a limited size of reduced separation, which is very similar to recent experiments of Smalyuk *et al.* [24]. The laser tweezers were also used for switching liquid crystal microdroplets [25], optical manipulation of defects in lyotropic liquid crystals [26], manipulation of islands on freely suspended smectic films [27], and for trapping and manipulation of high-index colloids in the nematic [28]. We should stress that the tweezers were used by Hotta and Masuhara to trap and manipulate defects in a nematic liquid crystal [29]. In those experiments, the underlying phenomenon is very similar to what we have observed in our experiments with low-index colloids in nematics, and two possible trapping mechanisms have been proposed.

Recently Muševič *et al.* [30] have reported an unusual mechanism of laser trapping and manipulation of small colloids in the nematic liquid crystal. In that experiment,

*Corresponding author. Email address: igor.musevic@ijs.si

micron-sized glass particles with homeotropic boundary conditions were dispersed in the nematic liquid crystal with refractive indices that were larger compared to the index of refraction of colloids. Under such conditions, a repulsive force is expected to arise between a strongly focused light and the colloidal particle. As a surprise, the opposite was clearly observed: the colloid was attracted into the laser focus (trap) over extraordinary large separations of several microns. Muševič *et al.* have observed that the optically induced distortion [i.e., optical Fréedericksz transition, (OFT)] of the nematic director field plays an important role, and two possible mechanisms were identified that are important in this forbidden trapping.

Below the OFT threshold, the forbidden trapping has its origin in the anisotropic dielectric coupling of the electric field of the electromagnetic (EM) wave with the director field around the colloid. Namely, the surface-induced distortion of the director field around the particle is accompanied by spatially varying direction of the eigenaxis of the dielectric tensor for optical frequencies. For a particular polarization of the trapping beam, there are two energetically favorable locations of the beam waist, where the polarization is directed along the long axis of the molecules. The colloid is, therefore, attracted into the laser focus until the favorable region of the distorted director field is in the most intense part of the optical trap. One could say, that "the particle is dressed with an anisotropic high-index cloud" and behaves effectively as a high-index particle compared to its surroundings.

Above the OFT threshold, the highly localized EM wave creates a localized region of a liquid crystal, which is elastically distorted. This optically induced distorted region, in principle, interacts with the colloid and can lead to an anisotropic interaction between the laser focus and the colloid. The mechanism of optical trapping is, therefore, accompanied by the elasticity-mediated interaction between two objects, the first object being the optically distorted region of a liquid crystal and the second object is the colloid. On the other hand, this can be considered as if the laser light "creates a ghost colloid at the laser focus" (for the reasons explained in Ref. [30]) that interacts via elasticity-mediated structural forces with the real colloid. It should be stressed that in both cases, the colloid is attracted into the optical trap indirectly and the direct interaction between the low-index colloid and the optical trap is repulsive.

In this paper, we elaborate in detail the two proposed mechanisms and compare the experimental results with theoretical predictions using a numerical approach. In the experimental part, we first give a detailed description of the laser tweezers experiments followed by an extensive analysis of the observed trajectories of the colloids during many trapping experiments for different laser power. This is followed by an extensive analysis of the laser trapping potential, which turns out to be highly anisotropic in space. For a certain range of colloidal separations and direction, we observe the Coulomb-like pair potential with an apparent $1/r$ separation dependence. In the theoretical section, we present a numerical study of the interaction of the colloidal particle with a strongly focused laser light, where the laser-induced local Fréedericksz transition is taken into account. We show that
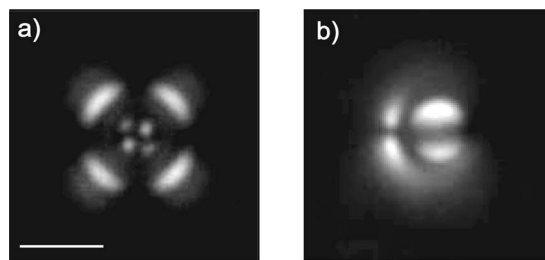

FIG. 1. (a) Polarization micrograph of a 4 μm diameter silica colloid treated with DMOAP in a homeotropic cell of 5CB. The dipolar field distribution around the colloid cannot be resolved, because the dipolar axis is along the director, i.e., perpendicular to the plane of the paper. The hedgehog is, therefore, either positioned above or below the colloid. The scale corresponds to 5 μm. (b) The same type of colloid in a planar 5CB cell clearly shows the dipolar director distribution. The same type of ordering is observed for 0.97 μm colloids.

this scenario reproduces an effective $1/r$ dependence of the trapping potential in a certain direction very well. The analysis shows that the Coulomb-like potential is reproduced only for a very specific direction of the pair potential and is a result of the combination of several interaction terms.

II. EXPERIMENT

The experiments have been performed using silica spheres of diameter $2a=(0.97\pm0.05)$ μm and the refractive index $n_s=1.43$ (measured at 590 nm) that were dispersed in a nematic liquid crystal $4'$-n-pentyl-4-cyanobiphenyl (5CB). The refractive indices of 5CB are $n_o=1.52$ and $n_e=1.69$ at room temperature measured at 1.064 nm [31]. Some of the experiments have also been performed in E12, which is an eutectic mixture of n-cyanobiphenyls with a clearing temperature of 59 °C. At room temperature and measured at 590 nm, the ordinary index of refraction of E12 is $n_o=1.52$ and the extraordinary index is $n_e=1.74$. As E12 is a mixture of n-cyanobiphenyls, we can expect that the refractive indices at 1064 nm are only slightly reduced (of the order of 0.01) and are, therefore, higher than the refractive index of silica spheres. We have also determined the temperature increase at maximum power used in the experiments, which is of the order of only 0.2 K. The corresponding changes of the refractive indices of a liquid crystal are, therefore, negligible.

The surface of the spheres was first covered with a monolayer of N,N-dimethyl-N-octadecyl-3-aminopropyl-trimethoxysilyl chloride (DMOAP) that ensures very strong homeotropic surface anchoring of a nematic liquid crystal. The particles were then introduced into the nematic liquid crystal and analyzed under the polarizing microscope. A typical image of somewhat larger (4 μm) colloidal particle in a 5CB homeotropic cell under crossed polarizers is shown in Fig. 1(a), whereas the same type of particle in a 5CB planar cell is shown in Fig. 1(b). We should comment that very similar structures were observed for 0.97 μm silanated silica colloids, only the image quality was worse.

The two images clearly show the dipolar character of the director field around the silanated colloids in the nematic,

and this dipolar configuration is observed for the majority of colloids used in the experiments. However, a more careful analysis shows that there is also a minority of colloids that show quadrupolar, saturnlike configuration of the surrounding nematic. This indicates an intrinsic distribution of the surface anchoring strength of our colloids, which has been considered in the interpretation of trapping experiments, discussed at the end of this section.

The nematic colloidal dispersion was heated into the isotropic phase, intensively sonicated to obtain homogeneous dispersion of isolated colloidal particles and then introduced into a glass cell using capillary force. When preparing the colloidal dispersion, the volume concentration of colloidal particles should be very low, of the order of 1 ppm. Such a low concentration prevents buckling of colloids during the cooling and phase transitions. We have used cells made of soda-lime glass plates of thickness 0.15 mm that were also covered with DMOAP to ensure good homeotropic alignment of the LC. Cells of different thicknesses were used in the experiments, ranging from 10 to 50 μm.

We have used a laser tweezers setup built around an inverted microscope (Zeiss, Axiovert 200 M), with a fast video camera and a cw diode-pumped solid-state laser (Coherent, Compass 2500 MN) at 1064 nm was used as a laser source. An acousto-optic deflector [(AOD) IntraAction, model DTD-274HA6)], driven by a computerized system (Aresis, Tweez Tek 70) was used for trap manipulation. A beam expander was used to match the laser beam to the AOD aperture and some additional optics were used to image the pivotal point of the AOD onto the entrance pupil of the water immersion microscope objective (Zeiss, IR Achroplan 63/0.9 W). The maximum laser power of a diffraction limited Gaussian beam in the sample plane was up to 64 mW. The laser light was linearly polarized and two orthogonal polarizations could be selected using a rotating half-wave plate. For a general review of the laser tweezers technique and experiments in soft condensed matter, the reader should refer to Ref. [32].

We have observed that colloids could be found at very different separations from the walls of the confining cell and were not attracted to the walls. This indicates a repulsion between the dipolar colloid and the homeotropic wall. We have first selected an isolated particle and the tweezers focus was positioned in the same plane close to the particle. The separation was set approximately to 10 μm, and the movement of the particle toward the laser focus was video monitored at a rate of 20 frames/s. We have observed that during the trapping experiments in thick cells (i.e., thicker than 10 μm), the image of the particles was slightly defocused during its approach to the laser trap, indicating that the particle does not stay in the same plane during the approach. We have estimated that the maximum off-plane deviation of the particles is less than 1 μm. We have also observed that the direction of the dipolar axis of the colloids does not deviate much during the trapping event. Slight changes in the direction of the dipolar axis, though, are observable.

Below the laser power for optical Fréedericksz transition (OFT), i.e., at low power levels, up to 30 mW for 5CB, the particle attraction was observed over separations of around 5 μm. By rotating the polarization of the optical trap, we have found that the particle was always attracted along the
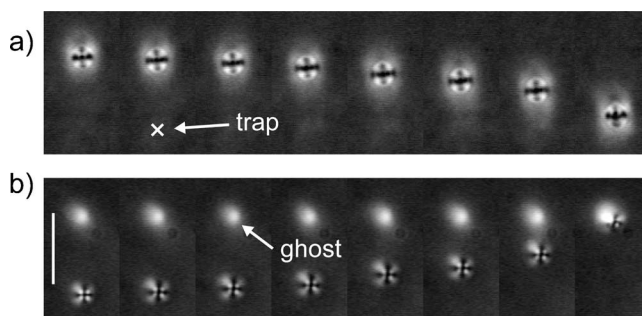

FIG. 2. Sequences of micrograph images under crossed polarizers, showing two different trapping events in 5CB, in a 50 μm thick cell. The scale bar is 10 μm and is equal for both images. The time steps are equal for both images. Note the apparent size of a 0.97 μm diameter colloid under crossed polarizers. (a) Trapping at low power of 25 mW, which is just below the power that is necessary to induce the local optical Fréedericksz transition (in this case, the threshold power is 30 mW). The cross indicates the position of the optical trap, which is not visible. (b) Trapping at 35 mW, which is above the optical Fréedericksz transition. The bright spot is due to a local birefringent area, created by the laser-light-induced distortion of the director field.

direction of polarization of the laser light. This is a clear indication that the particle is attracted into the laser trap via anisotropic dielectric interaction of the electric field of the EM and the inhomogeneous field of the dielectric tensor for optical frequencies. As we have already stressed in the introduction, due to a distorted director field in the close vicinity of the colloid, there is a region of enhanced refractive index for a given polarization of the laser beam with respect to homeotropic surroundings. The region of enhanced refractive index is positioned symmetrically with respect to the center of the colloid and there are two energy minima very close to the surface of the colloid where the colloid is trapped. This is difficult to observe on 1 μm colloids, but is very nicely resolved in the experiments with larger colloids. For example, in the experiments using 4 μm diameter low-index colloidal particles (not presented in this paper), we have clearly observed that the colloid is trapped precisely at the interface between the colloid and the liquid crystal.

Above the laser power for optical Fréedericksz transition (OFT), we have observed stronger trapping that was efficient over separations of more than 10 μm. Under unpolarized imaging, it appeared as if the colloid was attracted by another, invisible, i.e., "ghost," colloid positioned at the focus point. However, the nature of this ghost colloid was revealed by observing the trapping event under crossed polarizers, as shown in the series of polarized micrograph images in Figs. 2(a) and 2(b). Figure 2(a) shows a trapping event just below the threshold for Fréedericksz transition, where the position of the laser trapped cannot be resolved, as there is no optical-induced deformation of the director field. However, one can clearly see that when the laser power was increased above the Fréedericksz threshold, significant distortions of the director field around the laser focus were observed [bright spot in Fig. 2(b)]. This distorted region, therefore, acts as a long-range trapping site, attracting the particle over several micrometers. We are, therefore, in a regime, where the laser

trapping itself (i.e., the dielectric coupling of light and matter) is accompanied by liquid crystal elasticity-mediated interaction.

In an off-line analysis, the position of the center of gravity of the particle was determined by a computer video analysis of the captured frames with an accuracy of ±3 nm. Having the recorded time dependence of the separation between the particle and the laser focus, it was possible to restore the effective elastic pair potential between the particle and the laser trap. Following the Stokes law, the drag force $F = 6\pi R_{eff}\eta \partial r/\partial t$ is nearly balanced with the attractive force from the laser focus. The resulting unbalanced acceleration corresponds only to a fraction of both forces. The force between the focus of the laser tweezers and the silica particle was, therefore, calculated from the recorded time series of the particle's positions. Finally, by integrating the calculated drag force over the separation, we could determine the interaction pair potential. This analysis was performed on several tens of trapping experiments, leading basically to identical results.

In addition to trapping experiments, we have also performed a Brownian motion experiment, similar to Loudet *et al.* [33], where the product of the effective radius and viscosity $6\pi R_{eff}\eta$ could be determined. This was done simply by recording and analyzing Brownian motion of the colloid in the absence of the laser light. As an example, we show, in Fig. 3(a), the trajectory of the colloid in a homeotropic cell filled with 5CB during the time interval of 300 s, showing in total around 5000 recorded positions. The time interval τ between the two neighboring positions is $\tau = 61$ ms. Figures 3(b) and 3(c) show the corresponding histograms of particle displacements in two perpendicular directions. It is clearly a Gaussian distribution with a width of $2\sigma = 34(1\pm0.01)$ nm. The self-diffusion coefficient D of thermal motion is related to the width of the distribution σ and the time τ between two consecutive steps via $D = \sigma^2/\tau$ [33]. Finally by using Stokes-Einstein relation, we can determine the product of the effective radius and viscosity, which is in our case $R_{eff}\eta = 4.6\times10^{-8}$ kg s^{-1} for $2a = 0.97$ μm silanated silica spheres in 5CB at room temperature. We should note that this product can change slightly when the particle is in the distorted director field.

In all experiments performed and in the range of laser power above the optical Fréedericksz transition, we have observed basically two different types of trajectories of particles during the trapping event. These are shown in Figs. 4(a)–4(c). Figures 4(a) and 4(b) show the spiderlike trajectories that were observed in approximately 80% of the experiments. The starlike trajectories shown in Fig. 4(c) were observed in approximately 20% of our experiments, where, in total, more than 20 trapping experiments have been performed. The different symmetries of the two types of trajectory indicate two different symmetries of the director field around the colloid. We conclude that we have around 80% of the cases, where the director field has no mirror symmetry with respect to *x-y* plane (see Fig. 6) and 20% of the cases, where this mirror symmetry is observed. The first case indicates that strong colloidal surface anchoring induces dipolelike director distortion. The latter case most probably corresponds to the weaker surface anchoring, where quadrupolelike director distortion is realized.
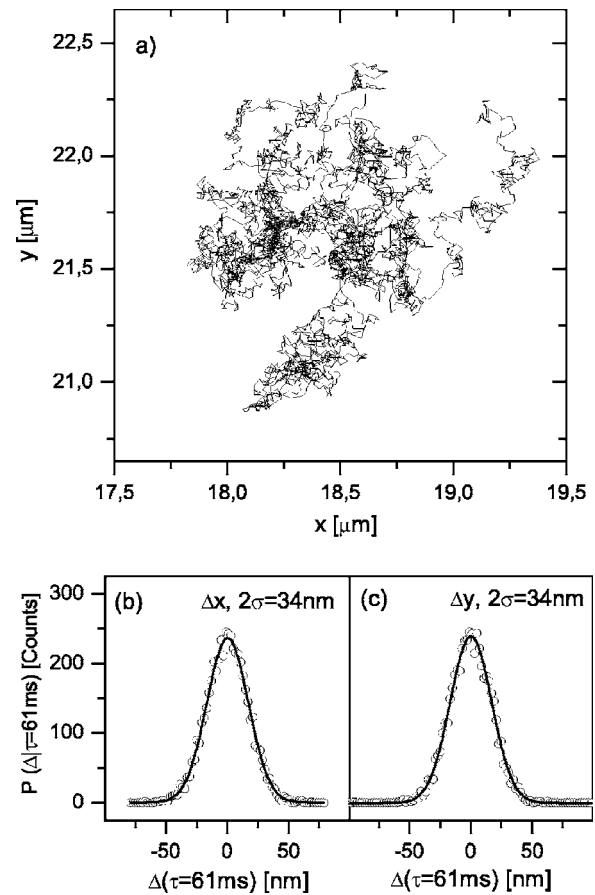

FIG. 3. (a) Recorded trajectory during the Brownian motion of a silanated 0.97 μm silica colloid in a homeotropic cell filled with 5CB. (b) and (c) represent histograms of particle's displacements between two consecutive positions, separated by a time interval of 61 ms, along the two perpendicular directions. The solid lines are Gaussian fits with $2\sigma = 34(1\pm0.01)$ nm. There is no difference between the *x* and *y* directions.

In order to answer these questions, several additional experiments have been performed. First, the DMOAP treated colloids were confined to a thin planar cell. We have clearly observed that a majority of colloids are indeed of dipolar type, corresponding to the strong surface anchoring. However, there was also a minority of colloids, that showed saturnlike geometry and even the configuration between the saturn and dipole, where the defect ring was not fully open, see Fig. 5. For a detailed description of the director field in the dipolar, saturn ring and intermediate configuration, the reader should refer to Fig. 5. in Ref. [11].

This is a clear proof of the heterogeniety of colloids and an indication of a certain distribution of the anchoring strengths on different colloids, although they were treated in the same way. Such a heterogeniety of surfaces is actually of no surprise to us and has been observed before in several microscale experiments on *LC* interfaces [34]. Second, trapping experiments have been performed in thin homeotropic cells, in order to see if the vicinity of the confining surfaces is responsible for different symmetries of the trajectories. We have found that there is no difference between the trapping trajectories in thin and thick cells.
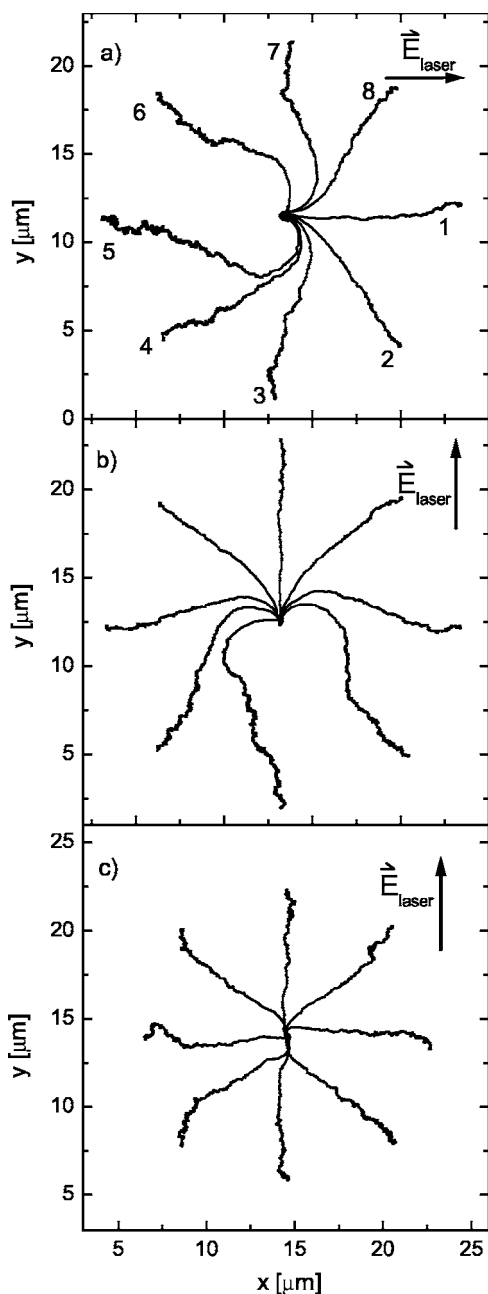
FIG. 5. (a) Optical micrograph of a pair of 4 μm silanated colloids in a planar cell of 7 μm thickness. The colloid on the left side is of dipolar type, whereas the colloid on the right side has a nearly fully open defect, which is close to the saturn ring configuration. (b) The same pair of colloids as seen under crossed polarizers.

the center. Clearly, the silica particles follow the shortest trajectory toward the laser focus only for certain directions, which we call an "easy direction." In other cases, there is a direction where the silica and ghost particles demonstrate repulsive interaction. In this case of a "hard direction," the particle avoids repulsion and takes a "detour" trajectory that ends in the laser focus. More precisely, measurement on larger (4 μm) colloids indicates that the position of the center of the trap is very close to the surface of the colloid, where the repulsion due to smaller index of refraction of the silica colloids becomes important. After changing the direction of polarization of the trapping beam, the set of trajectories is rotated by 90° as a whole. Since the polarization defines the two equivalent directions, whereas, we observe only one particular direction, one may conclude that the interaction depends on the exact deformation of the director produced by the laser irradiation.

III. THEORY

As our experiments clearly indicate, two types of laser trapping mechanisms for low refractive index colloids in a nematic liquid crystal, it is clear that we have to consider very carefully all the relevant fields and their couplings in the experimental geometry, shown in Fig. 6. In our theoretical approach, described in this section, we have considered: (i) propagation of focused laser light in a birefringent medium, (ii) all relevant distortions of the director field induced by strongly focused laser light, and (iii) all relevant couplings of the director field in the experimental geometry shown in Fig. 6(a) for the dipolar and Fig. 6(b) for quadrupolar colloid. The laser focus and the colloid were positioned in the same plane at the center of the cell. Also, the orientation of the dipolar field of the colloid was fixed during the approach to the trap. This is a rather complete description of the effective electroelastic potential that acts on a colloidal particle close to the laser trap. We expect that it can predict laser trapping below as well as above the optical Fréedericksz transition.

The calculation is based on a numerical integration of the free energy density consisting of three contributions: (i) elastic interaction due to deformed nematic director field around the colloid and the trap (Frank's elasticity), (ii) the dielectric interaction of an inhomogeneous and anisotropic director field with an inhomogeneous electric field of the focused light, and (iii) the repulsive dielectric interaction of a colloid

FIG. 4. (a) Spiderlike trajectories during the optical trapping of a 0.97 μm silica colloid in a 15 μm homeotropic 5CB cell. The laser power is 35 mW (i.e., above the optical Fréedericksz transition) and the starting positions are labeled 1–8. (b) The set of spiderlike trajectories rotates as a whole, as the polarization of the laser light is rotated by 90°. (c) Trapping of the same type of colloid at the same laser power, in a thicker 50 μm cell, that is observed in approximately 20% of the experiments. The spiderlike trajectories correspond to dipole director field around the colloid; whereas, the starlike trajectories shown in (c) indicate quadrupole symmetry of the director field around the colloid.

In this paper, we study in detail more abundant cases with spiderlike trajectories shown in Figs. 4(a) and 4(b) that are observed above the optically induced local Fréedericksz transition. The silica particle was released from the positions labeled 1–8 in a random sequence and the laser spot was in
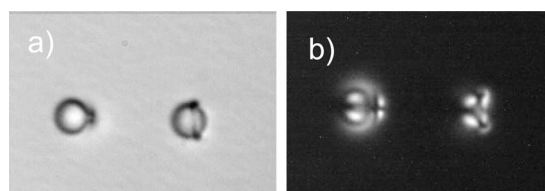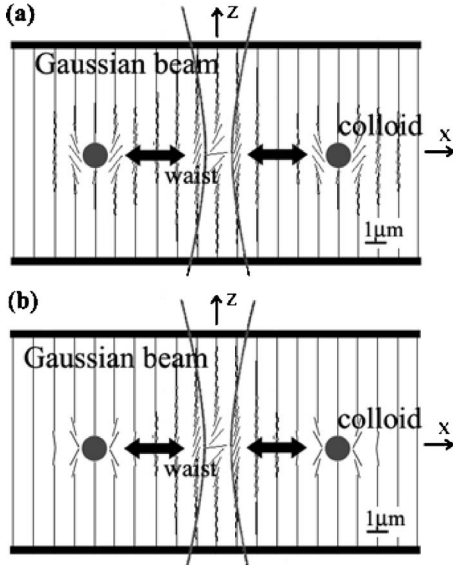
FIG. 6. Schematic of the interaction of a Gaussian light beam with a colloid in a homeotropic nematic cell. The beam induces an optical Fréedericksz transition, which creates a region of a distorted director field inside the cell. This can be considered as a ghost colloid that interacts with a real colloid. For convenience, the position of the colloid is set in the center of the cell; whereas, in the experiment, they can be found everywhere in the cell except close to the surface. Panel (a) shows the dipolar symmetry of the colloid and (b) shows the quadrupolar one.

(with a small refractive index) with an inhomogeneous electric light field. Till now, each of these interactions has been studied separately in a qualitative treatment [35,36].

The complete problem would be far too demanding to solve, so the one elastic constant approximation was used, which is well justified, as in 5CB, the elastic constants differ for at most ~40% [37]. The corresponding free energy is

$$F = -\frac{1}{2}K\int_{D^{LC}}\left(\frac{\partial n_i}{\partial x_j}\right)\left(\frac{\partial n_i}{\partial x_j}\right)dV - \frac{1}{2}\epsilon_a\epsilon_0\int_{D^{LC}}[\mathbf{n}(\mathbf{r})\cdot\mathbf{E}(\mathbf{r})]^2 dV$$

$$+ \frac{1}{2}(\epsilon_{LC}-\epsilon_C)\epsilon_0\int_{D^C}\mathbf{E}(\mathbf{r})^2 dV, \qquad (1)$$

where K is the average elastic liquid crystal constant, $\mathbf{r} = (x,y,z)$ is the position vector and x, y, and z are the corresponding Cartesian coordinates, $\mathbf{n}(\mathbf{r})$ is the director field, $\mathbf{E}(\mathbf{r})$ is the electric field of the laser trap, ϵ_C is the dielectric constant of the colloid, $\epsilon_a = \epsilon_\parallel - \epsilon_\perp$ is the liquid crystal dielectric anisotropy for optical frequencies, and $\epsilon_{LC} = (2\epsilon_\perp + \epsilon_\parallel)/3$ is the corresponding average dielectric constant of the liquid crystal for optical frequencies. In Eq. (1), the first two terms are integrated over the whole volume of the liquid crystalline medium (D^{LC}), while the third term is integrated over the volume of the colloid (D^C). Summation over repeated indices i,j is assumed.

Here we have considered that the electric field of the laser trap, which interacts with the liquid crystal, is time independent. This is well justified since the modulation frequency of the laser trap electric field is in the range of ~10^{14} Hz, while

the 5CB director switching rate is at its highest in 10^3 Hz range. In the calculation of the dielectric coupling of the colloid, the average liquid crystal dielectric constant for optical frequencies ϵ_{LC} is used. Ordinary and extraordinary dielectric constants in 5CB differ for ~10% from the average value. For a more precise analysis, the Mie scattering or other similar approaches should be used [38].

We have first determined the electric and the director fields for different positions of the colloid and the trap. The Gaussian beam profile has been used, which is a typical description for strongly focused laser beams [36]. The electric field $\mathbf{E}(\mathbf{r})$ of the focused light beam is

$$\mathbf{E} = \frac{\mathbf{E}_0}{\sqrt{\left(1+\left(\frac{z}{z_0}\right)^2\right)}}\exp\left(-\frac{x^2+y^2}{w_0^2\left[1+\left(\frac{z}{z_0}\right)^2\right]}\right). \qquad (2)$$

Here, $\mathbf{E}_0$ is the electric field amplitude of the linearly polarized light, w_0 is the radius of the waist, and $z_0 = \pi w_0^2 \sqrt{\epsilon_{LC}}/\lambda$ is the measure of the near (electric) field area, where λ is the wavelength of the laser light.

Note that the Gaussian beam profile [Eq. (2)] can be used only if refractions due to difference in refractive index of the liquid crystal and cell walls are negligible and if the laser beam impinges mostly along the optical axis. In our experiment, both conditions are justified. We have used glass cell walls with the refractive index of 1.5 and at the cell surfaces, homeotropically aligned 5CB, which has the same ordinary refractive index (the possible difference is less than a few percent). The effect of the anisotropic director field on the polarization is separately discussed later, let us just stress here that this simple approach with the Gaussian beam gives good results for distances between laser trap and the colloid larger than ~2–3 colloid radii.

The director field has been determined in two steps. First, the director field around the optical trap was numerically calculated using the Euler-Lagrange free energy minimization equations for the director field within a Gaussian beam [Eq. (2)]. Here, we have considered a local Fréedericksz transition induced by intense light in the presence of homeotropic boundary conditions at the confining plan-parallel walls of the sample cell with very strong surface anchoring. In the second step, the director field of the optical trap (ghost colloid) was combined with the dipolar ansatz (dipolar approximation) for the director field $\mathbf{n}$ around a spherical colloid with radius a and homeotropic anchoring $\mathbf{n}_{\mathbf{col}} \sim 3.08a^2(\mathbf{r}-\mathbf{R})/|r-R|^3$, which was discussed by Stark *et al.* in Ref. [39]. Here $\mathbf{R} = (X,Y,Z)$ stands for the position vector of the colloid. Finally, the combined normalized director field was used in the calculation of the free energy F. Schematic of the Gaussian beam and the director field with the ghost and real colloid is given in Fig. 6. Note the difference in the interaction for two opposite positions of the colloid. The director field of the colloid on the left side nearly matches the trap; whereas, there is strong distortion and, consequently, repulsion for the colloid approaching from the right side. Note that there is no such difference for the interaction for colloids with the quadrupolar director field.

Calculation of the combined director field as a normalized superposition of two contributions is well justified only at separations between the real and ghost colloid larger than a few a. Dipolar ansatz $\mathbf{n}_{col}$ is namely derived from a far-director field multipole expansion and this expansion is, in our particular geometry, valid only if X and Y components of the final director are small. In our calculations, this condition can be questionable at separations $|\mathbf{r}-\mathbf{R}| \lesssim 3a$, but, nevertheless, a later comparison between numerical and experimental results show that the dipolar ansatz gives reasonably good results also at small separations $\sim 2a$. A more general approach in calculation of the final director field would demand a minimization of proper tensorial liquid crystal free energy with homeotropic boundary conditions on the cell and colloid surfaces.

One could argue that the use of a linear polarization in the Gaussian beam is a very rude approximation since liquid crystals are well-known birefringent materials that split light beams in ordinary and extraordinary rays. Nevertheless, this is relevant only when the real and ghost colloid are very close (2–3 colloid radii) and the director can thus point in an arbitrary direction. When the real colloid is further away, the director and, consequently, the optical axis stay in the polarization plane. The light beam of the laser trap "feels" only extraordinary refractive index and, therefore, only slightly deflects from its incident direction. In our particular experiment, this "beam-walkoff" effect is, therefore, very small and the light beam deviates for less than 0.5 μm when passing through the whole cell ($\sim$20 μm thick). The polarization thus stays linear and mainly unperturbed.

IV. RESULTS AND DISCUSSION

Figure 7(a). shows the measured time dependence of the separation between the colloid and the laser trap at $P=50$ mW, when the colloid was released along the easy direction, starting from the position 1 in Fig. 4(a). The inset to Fig. 7(a) shows the log-log plot of the same data, clearly indicating the power-law dependence with an exponent $\alpha = 0.33(1 \pm 0.02)$. It can be shown that the exponent α describing the time dependence of the separation $r(t)=A(t_{max}-t)^{\alpha}$ is related to the exponent β describing the separation dependence of the pair potential $W_p = W_0 r^{\beta}$ through $\beta = 2-(1/\alpha)$ [33]. For $\alpha = 0.33(1 \pm 0.02)$ this gives Coulomb-like attraction with an exponent $\beta = -1.01(1 \pm 0.05)$. An extensive analysis of a set of several experiments on different samples and colloids basically confirms this Coulomb-like attraction with an average exponent of $\beta = -0.99(1 \pm 0.06)$.

The separation dependence of the interaction between the colloid and the laser trap was also analyzed by calculating the separation dependence of the attractive force. After integrating the force over separation, the pair potential was calculated, as shown in Fig. 7(b). The potential is of the Coulomb-like type, as evidenced by a very good fit indicated by a solid line. The potential is extremely strong, reaching several thousands of k_BT at small separations. We have also analyzed the strength W_0 of the trapping potential as a function of the optical power in the trap, which is shown in
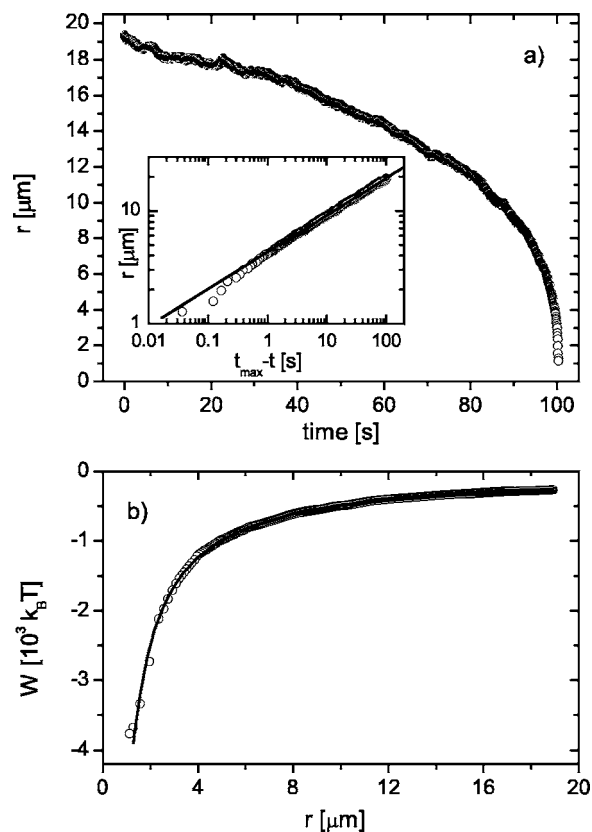

FIG. 7. (a) Recorded time dependence of the separation between a silica particle and the laser trap during the trapping event in a 15 μm homeotropic 5CB cell at a laser power of 50 mW, starting from the "easy position" labeled 1 in Fig. 4(a). The colloid is trapped at a time labeled t_{max}. The inset shows the log-log plot of the same data showing clear power-law dependence with an exponent $\alpha = 0.33(1 \pm 0.02)$. (b) The laser trapping potential derived from the data in (a). The solid line is the best fit to $W(r)=W_0/r$ with $W_0 = 5980(1 \pm 0.002)k_BT$ μm.

Fig. 8. The discontinuity at the Fréedericksz transition at 30 mW is observable.

Let us now compare the experimental data to the numerical calculations of the resulting effective potential of our
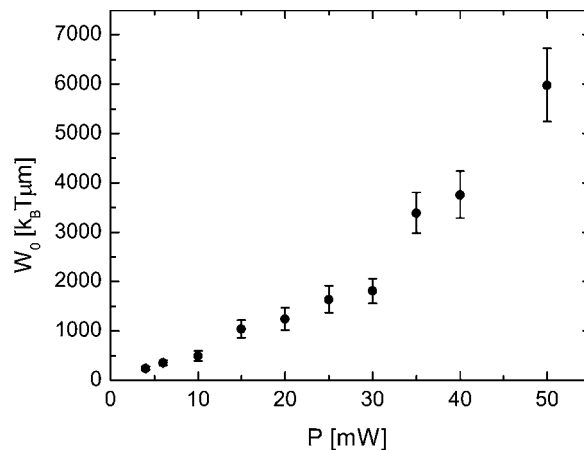

FIG. 8. The strength of the trapping potential along the easy direction as a function of the optical power.
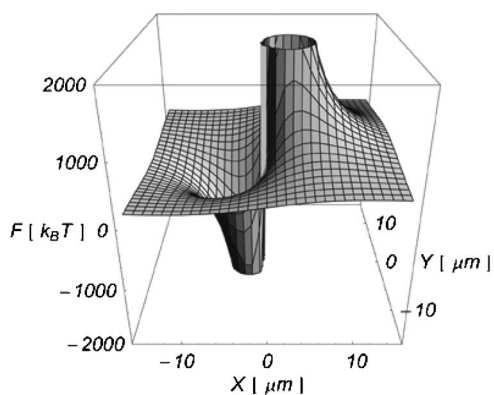
FIG. 9. The effective pair potential for the colloid in the vicinity of the laser trap at large laser power, i.e., above the local Fréedericksz transition. The trap is centered at $X=Y=0$, the light polarization is along the x direction. The cell thickness is 20 μm, $K=6\times10^{-12}$ N, $\epsilon_{\parallel}=2.9$, $\epsilon_{\perp}=2.3$, $\mathbf{E}_0=(8\times10^6 \text{ V/m})\mathbf{e_x}$, $w_0=0.5$ μm, $\lambda=1064$ nm, $a=0.5$ μm, and $\epsilon_C=1.7$.

optical trap, which are presented in Figs. 9 and 10. The laser Gaussian beam propagates along the z axis at $X=Y=0$. The values of the pair potential are calculated in the $Z=0$ plane positioned at the separation 10 μm from the cell wall (see Fig. 6).

Figure 9 represents the numerically calculated trapping potential above the local optically induced Fréedericksz transition. One can see that numerical calculations reasonably well explain the observed trajectories of the colloid trapping, shown in Fig. 4. In most of the XY plane, the colloid experiences an attractive potential of the optical trap that attracts it in a nearly straight line toward the trap. The starting point labeled 1 in Fig. 4(a), therefore, corresponds to the laser trapping from the left side of the potential well in Fig. 9. However, as the numerically calculated potential is of an asymmetrical shape, the colloid is deflected from the straight direction, if it approaches the trap from the hard direction. This is a direction from the far right side of the potential well in Fig. 7 that corresponds to the position 5 in Fig. 4(a).
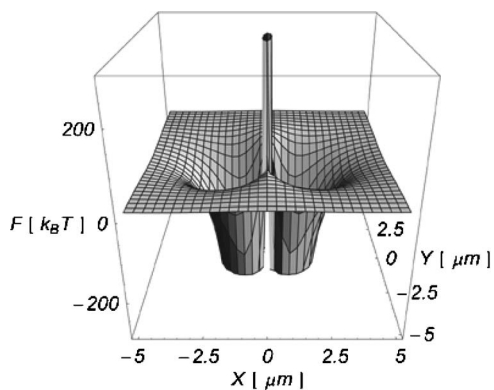

FIG. 10. The effective potential for the colloid approaching the laser trap below the local Fréedericksz transition. The trap is centered at $X=Y=0$, the light polarization is along the x direction. The following parameters were used in numerical calculation: $K=6\times10^{-12}$ N, $\epsilon_{\parallel}=2.9$, $\epsilon_{\perp}=2.3$, $\mathbf{E}_0=(3\times10^6 \text{ V/m})\mathbf{e_x}$, $w_0=0.5$ μm, $\lambda=1064$ nm, $a=0.5$ μm, and $\epsilon_C=1.7$

We have fitted the effective free energy F with a power law a_0+b_0/r_i^{α}, where i stands for X or Y and a_0,b_0 are constants. Along the easy direction (-15 μm $<X<-1$ μm, $Y=0$), we find $\alpha=1.1$, which is close to the observed Coulomb-like exponent. Over the range of separation ($X=-1$ μm, $0<|Y|<15$ μm), we find $\alpha=1.6$. Note that in the direction perpendicular to the polarization the attractive potential decays with a higher exponent, which is due to the anisotropy of the director field to electric field.

Numerical results of the potential strength are also in a rather good agreement with the experiment. Along the easy direction, the potential drops to a minimum value of $\sim3000k_BT$ compared to zero potential far away, which is in good agreement with experimental values, see Fig. 6(b). As a result, this potential drop gives rise to a typical 1 pN force. We should stress that the strength of the potential depends strongly on the laser power; whereas, its shape changes substantially only when the laser power is above the threshold for the local optical Fréedericksz transition (see Figs. 9 and 10).

Figure 10 shows the trapping potential at a low power level, i.e., below the optical Fréedericksz transition. The remaining asymmetry in the effective pair potential at low laser power is caused by the anisotropic dielectric director to electric field interaction. Along the direction of the polarization, this interaction is stronger as in the perpendicular direction, which results in two potential minima positioned symmetrically along the direction of polarization. The reason is in the director field in the close vicinity of the colloid, which is parallel to the light polarization only in two localized regions close to the colloidal surface.

Finally, we should emphasize that the observed Coulomb-like exponent for the attraction along the easy direction is a result of a combination of several interactions: (i) the elastic anisotropic attraction between the laser-distorted nematic in the laser waist and the elastically deformed region around the colloid, (ii) the anisotropic dielectric attraction of the laser polarization with distorted and optically anisotropic nematic, and (iii) the symmetric and repulsive interaction between the low-index colloid and the laser waist. The combination of these three interactions gives rise to an effective Coulomb-like attraction. We should stress that this type of interaction is observable only for a certain direction; whereas, in other directions, the effective exponent of the pair potential is quite different and even changes sign.

In order to give a more quantitative insight into contributions of different mechanisms, the corresponding free energies are plotted separately in Fig. 11. In both high and low laser power regimes, one can see that the main contribution to the effective potential F comes from the dielectric interaction. At shorter distances ($|X|\lesssim1$ μm), dielectric coupling between the colloid and the electric field is important, while at larger distances ($|X|\gtrsim2$ μm), dielectric coupling between the inhomogeneous electric and inhomogeneous director field governs the trapping of the colloid. Elastic interaction is at a laser power above the OFT value at all separations X smaller as the dielectric coupling; however, it still affects the details of the power-law dependence of F.

Furthermore, we should stress the importance of the influence of the confining walls and their surface anchoring. As
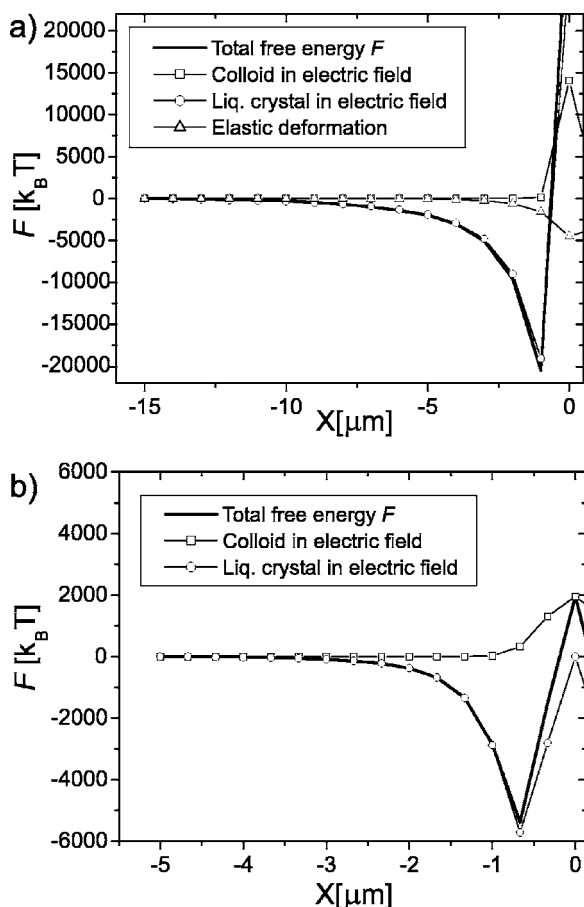
FIG. 11. Contributions of different interactions [see Eq. (1)] to the total effective potential that acts on a colloidal particle within the electric field of the optical trap for laser power. Results are presented in the easy direction for laser powers: (a) above the optical Fréedericksz transition (OFT) value, (b) below the OFT value. Note the dominating contribution of the dielectric interaction at larger separations.

a general rule, we can expect that the anchoring at the confining walls has an effect of screening on the interaction potential F for trap-particle separations that are comparable to the particle-wall separation. Therefore, for trap-particle separations smaller than the particle-wall separation, power-law dependence in F is expected. On the other hand, for larger trap-particle separations, the potential F is expected to decay exponentially, with the characteristic length that is equal to the particle-wall separation.

V. CONCLUSIONS

In conclusion, we have presented and analyzed the laser trapping of small colloidal particles dispersed in nematic liquid crystals, when their refractive index is low compared to the refractive indices of a liquid crystal. At low laser power, that is below the optical Fréedericksz transition, the colloid is trapped via its "birefringent cloud." At high laser power, the optical trapping is accompanied by the interaction between the laser-induced distortion of a director field and the colloid. In this regime, we have observed two different types of trapping trajectories. The first type of trajectory is highly anisotropic, spiderlike, and has been observed in approximately 80% of the trapping experiments. The symmetry of the trajectories is consistent with a simple picture, where a colloid with its dipolar director field is attracted into the localized, highly distorted nematic field in the laser trap. Depending on the direction of the polarization of the light field, there is an easy direction, where the colloid is attracted by an apparent, Coulomb-like pair potential. A numerical analysis, where the elastic anisotropic attraction between the laser-distorted nematic and the deformed region, the anisotropic dielectric attraction of the laser polarization with distorted and optically anisotropic nematic, and the symmetric and repulsive interaction due to low refractive index of the colloid are considered, shows good qualitative agreement with experiments. It clearly shows, that the apparent, Coulomb-like interaction is a result of the combination of these three interaction terms. We should also stress that screening of the laser trap-colloid interaction due to the presence of the confining walls should also be considered above a certain range of separation. Finally, the symmetry properties of approximately 20% of the trapping trajectories indicate a quadrupolar director field around the colloids. This type of ordering has already been observed in other experiments [40], and the numerical analysis of trapping of quadrupolarlike colloids is left for possible future studies. Nevertheless, it should be stressed that already a selected choice of the experiments and their analysis show that there are subtle force mechanisms that have to be carefully considered in laser tweezers experiments in soft matter.

ACKNOWLEDGMENTS

[1] P. Poulin, H. Stark, T. C. Lubensky, and D. A. Weitz, Science **275**, 1770 (1997).

[2] P. Poulin and D. A. Weitz, Phys. Rev. E **57**, 626 (1998).

[3] Y. Ch. Loudet, P. Barois, and P. Poulin, Nature (London) **407**, 611 (2000).

[4] V. G. Nazarenko, A. B. Nych, and B. I. Lev, Phys. Rev. Lett. **87**, 075504 (2001).

[5] I. I. Smalyukh, S. Chernyshuk, B. I. Lev, A. B. Nych, U. Ognysta, V. G. Nazarenko, and O. D. Lavrentovich, Phys. Rev. Lett. **93**, 117801 (2004).

[6] M. Yada, J. Yamamoto, and H. Yokoyama, Langmuir **18**, 7436 (2002).

[7] S. P. Meeker, W. C. K. Poon, J. Crain, and E. M. Terentjev, Phys. Rev. E **61**, R6083 (2000).

[8] S. L. Lopatnikov and V. A. Namiot, Zh. Eksp. Teor. Fiz. **75**, 361 (1978) [Sov. Phys. JETP **48**, 180 (1978)].

[9] S. Ramaswamy, R. Nityananda, V. A. Raghunathan, and J. Prost, Mol. Cryst. Liq. Cryst. Sci. Technol., Sect. A **288**, 175 (1996).

[10] O. V. Kuksenok, R. W. Ruhwandl, S. V. Shiyanovskii, and E. M. Terentjev, Phys. Rev. E **54**, 5198 (1996).

[11] T. C. Lubensky, D. Pettey, N. Currier, and H. Stark, Phys. Rev. E **57**, 610 (1998).

[12] B. I. Lev and P. M. Tomchuk, Phys. Rev. E **59**, 591 (1999).

[13] S. B. Chernyshuk, B. I. Lev, and H. Yokoyama, Zh. Eksp. Teor. Fiz. **120**, 871 (2001) [JETP **93**, 760 (2001)].

[14] B. I. Lev, S. B. Chernyshuk, P. M. Tomchuk, and H. Yokoyama, Phys. Rev. E **65**, 021709 (2002).

[15] H. Stark, Eur. Phys. J. B **10**, 311 (1999).

[16] H. Stark, Phys. Rep. **351**, 387 (2001).

[17] D. Andrienko, G. Germano, and M. P. Allen, Phys. Rev. E **63**, 041701 (2001).

[18] D. Andrienko, M. P. Allen, G. Skačej, and S. Žumer, Phys. Rev. E **65**, 041702 (2002).

[19] O. Guzman, E. B. Kim, S. Grollau, N. L. Abbott, and J. J. de Pablo, Phys. Rev. Lett. **91**, 235507 (2003).

[20] Jun-ichi Fukuda, M. Yoneya, H. Yokoyama, and H. Stark, Colloids Surf., B **38**, 143 (2004).

[21] Jun-ichi Fukuda, H. Stark, M. Yoneya, and H. Yokoyama, Phys. Rev. E **69**, 041706 (2004).

[22] P. Poulin, V. Cabuil, and D. A. Weitz, Phys. Rev. Lett. **79**, 4862 (1997).

[23] M. Yada, J. Yamamoto, and H. Yokoyama, Phys. Rev. Lett. **92**, 185501 (2004).

[24] I. I. Smalyukh, A. N. Kuzmin, A. V. Kachynski, P. N. Prasad, and O. D. Lavrentovich, Appl. Phys. Lett. **86**, 021913 (2005).

[25] S. Juodkazis, M. Iwashita, T. Takahashi, S. Matsuo, and H. Misawa, Appl. Phys. Lett. **74**, 3627 (1999); S. Juodkazis, S. Matsuo, N. Murazawa, I. Hasegawa, and H. Misawa, Appl. Phys. Lett. **82**, 4657 (2003).

[26] Y. Iwashita and H. Tanaka, Phys. Rev. Lett. **90**, 045501 (2003).

[27] A. Pattanaporkratana, C. S. Park, J. E. Maclennan, and N. A. Clark, Ferroelectrics **310**, 131 (2004).

[28] T. A. Wood, H. F. Gleeson, M. R. Dickinson, and A. J. Wright, Appl. Phys. Lett. **84**, 4292 (2004).

[29] Jun-ichi Hotta and H. Masuhara, Appl. Phys. Lett. **71**, 2085 (1997).

[30] I. Muševič, M. Škarabot, D. Babič, N. Osterman, I. Poberaj, V. Nazarenko, and A. Nych, Phys. Rev. Lett. **93**, 187801 (2004).

[31] Jun Li and Shin-Tson Wu, J. Appl. Phys. **95**, 896 (2004).

[32] Paras N. Prasad, *Introduction to Biophotonics* (Wiley, New York, 2003).

[33] J. C. Loudet, P. Hanusse, and P. Poulin, Science **306**, 1525 (2004).

[34] I. Muševič and K. Kočevar, in *Surfaces and Interfaces of Liquid Crystals*, edited by Th. Rasing and I. Muševič (Springer-Verlag, Berlin, 2004).

[35] P. G. de Gennes and J. Prost, *The Physics of Liquid Crystals*, 2nd ed. (Oxford Science Publications, Oxford, 1993).

[36] T. Tlusty, A. Meller, and R. Bar-Ziv, Phys. Rev. Lett. **81**, 1738 (1998).

[37] G. Chen, H. Takezoe, and A. Fukuda, Liq. Cryst. **5**, 341 (1989).

[38] H. C. Van de Hulst, *Light Scattering by Small Particles* (John Wiley & Sons, New York, 1957).

[39] H. Stark, habilitationsschrift, University of Stuttgart, 1999 (unpublished).

[40] Yuedong Gu and N. L. Abbott, Phys. Rev. Lett. **85**, 4719 (2000).